Journal of Thermal Analysis and Calorimetry, Vol. 84 (2006) 1, 147–155

# EFFECT OF INTERLAYER CATIONS ON HIGH-TEMPERATURE PHASES OF VERMICULITE

*V. Ramírez-Valle*[1], *M. C. Jiménez de Haro*[1], *M. A. Avilés*[1], *L. A. Pérez-Maqueda*[1], *A. Durán*[1], *J. Pascual*[2] *and J. L. Pérez-Rodríguez*[1*]

[1]Instituto de Ciencia de Materiales de Sevilla. CSIC-Universidad de Sevilla. C/Américo Vespucio s/n. 41092 Sevilla, Spain
[2]Departamento de Ingeniería Civil, Materiales y Fabricación, ETSII, Universidad de Málaga, Campus El Ejido, 29013 Málaga, Spain

Static and dynamic heating of vermiculite samples from Santa Olalla, Huelva, Spain, saturated with different cations, i.e. $Na^+$, $Cs^+$, $NH_4^+$, $Mg^{2+}$, $Ca^{2+}$, $Ba^{2+}$ and $Al^{3+}$, have been studied. The characterization of the phases formed during heating has been carried out by X-ray diffraction. The phases formed depend on the cation present in the interlamellar position and the heating process. The phases identified in the vermiculite samples saturated with different cations and heated at different temperatures are the following: enstatite, forsterite, spinel, cordierite, anorthite, pollucite, nepheline, coesite, celsian and others various mixed silicates; also some dehydrated and amorphous phases have been observed. On static heating, at the maximum temperature reached in this work, the phases formed appear mixed with a glassy phase.

***Keywords:*** *anorthite, celsian, coesite, cordierite, enstatite, forsterite, interlayer cation, nepheline, pollucite, spinel, thermal behaviour, vermiculite*

## Introduction

Vermiculite is a mineral of significant practical importance [1, 2] which structure consists of unit layer composed of two silica tetrahedral sheets with a central magnesium octahedral sheet. Vermiculite contains Al for Si substitution in its tetrahedral layers and Al–Fe for Mg substitutions in octahedral, these substitutions are responsible of the negative charge of the structure, that is compensated by exchangeable cations.

When raw vermiculite flakes are strongly heated at high temperature (≈900°C) during a short period of time, the water situated between layers is quickly converted into steams, exerting a disruptive effect upon the structure. As a consequence, a highly porous exfoliated material, which is an efficient thermal insulator, is formed [3–7]. This material presents excellent refractory properties, melting point at 1315°C and sintering temperature of 1260°C [8].

The service temperature of exfoliated vermiculite bonded to form bricks is limited by the shrinkage of bond, but not by friability [9]. The usage of vermiculite as raw material in order to obtain new glassed and vitro-crystalline or vitroceramic materials has been studied by Rincon [10, 11]. Podebradska *et al*. [12] have recently reported that the application of vermiculite aggregates instead of sand in reinforced cement composites is clearly positive because of its porous character leading to the bulk density decrease without worsening other properties.

The nature of hydration of vermiculite saturated with different cations can be revealed by Thermal Analysis (thermogravimetric and differential thermal analysis). Barshad [13] showed that, when $Ca^{2+}$ and $Mg^{2+}$ are the exchangeable cations there is a double layer of water, when the exchangeable cations are $Ba^{2+}$ and $Na^+$ there is a single layer of water and when $NH_4^+$ and $Cs^+$ are the exchangeable cations the vermiculite has no interlayer water. The sizes and complexities of the initial peaks for vermiculite with any of these ions vary in accordance with hydration characteristics of the particular cation present. Differences in hydration/dehydration behaviour of vermiculite saturated with diverse cations are well described in literature [13, 14]. Vermiculite starts to evolve its hydroxyl water at about 600°C being completely removed at 750°C, appearing an endothermic effect; this is followed by an exothermic effect at about 850°C [13, 15, 16]. The endothermic effect may be associated with some entropy change, while the exothermic one is due to the recrystallization into new phases [16]. The influence of the exchangeable cations present in the vermiculite on the thermal behaviour of the samples has been analyzed by TG, DTA and ETA thermal methods [17–19]. Ammonium vermiculites have been recently characterized by TG-MS hyphenated technique [20].

* Author for correspondence: jlperez@icmse.csic.es

1388–6150/$20.00

Akadémiai Kiadó, Budapest, Hungary
Springer, Dordrecht, The Netherlands

The high-temperature phases formed on the ignition of vermiculite have not been studied in detail. Walker [21] showed the formation of enstatite at about 800°C in his samples. Stoch [22] has reported that during crystallization of $MgO–Al_2O_3–SiO_2$ glasses, crystal phase formation is determined by the glass structure decomposition progress and its particular components release accompanying increase of temperature. In the case of vermiculite, the high temperature phases could be expected to show considerable variation, depending on lattice substitutions and exchangeable ions. Therefore, the phases formed on heating saturated-vermiculite during static and dynamic heating are not well known. Also the effect of exchange cations on the formation of these phases is unknown. Thus, the aims of this work are to study the thermal transformation and phases formed under dynamic and static heating of vermiculite saturated with $Na^+$, $Cs^+$, $NH_4^+$, $Mg^{2+}$, $Ca^{2+}$, $Ba^{2+}$ and $Al^{3+}$ up to 1450°C.

## Experimental

### *Materials*

Vermiculite from Santa Olalla (Huelva, Spain) was used, having a half-unit cell composition of $(Si_{2.64}Al_{1.36})(Mg_{2.48}Fe^{+}_{0.324}Fe^{2+}_{0.036}\ Al_{0.14}Ti_{0.01}Mn_{0.001})\ O_{10}\ (OH)_2\ Mg_{0.439}$ [23].

Vermiculite powder (<80 μ) was obtained using a Restch knife mill. Powder samples were saturated with different cations ($Na^+$, $Cs^+$, $Mg^{2+}$, $Ca^{2+}$, $Ba^{2+}$, $Al^{3+}$), by treatment with the corresponding ion-chlorine solution and heated under refluxing conditions; the procedure was repeated until the total cation exchange. The exception to this procedure was the $NH_4^+$ saturation, that consisted of obtaining a suspension of vermiculite in 1M $NH_4CH_3COO$ solution by agitation, this suspension was left to stand for 24 h and after centrifugation the process was repeated several times to achieve complete $NH_4^+$ exchange. All the saturated samples were finally washed with deionised water to eliminate $Cl^-$ and $CH_3COO^-$ respectively.

In order to check the total saturation in the different cations, an X-Ray diffraction analysis was realized to each sample of saturated-vermiculite.

### *Methods and samples characterization*

To study the thermal behaviour, the samples were annealed for 1 h at different temperatures, i.e. 900, 1000, 1100, 1200, 1300, 1330, 1400 and 1450°C, using a Carbolite Furnace Model RHF 1600; the heating rate was 5°C $min^{-1}$ and the maximum heating temperature used for each sample was determined by their melting point. X-ray diffraction study of the diverse phases formed was carried out using a Diffractometer-Kristalloflex D-501 Siemens at 36 kV and 26 mA with Ni filtered, $CuK_\alpha$ radiation and a graphite monochromator; the scanning rate used was 1° (2θ), between the range 2–70 (2θ) and with time constant of 1 s.

Additionally, the samples were heated from room temperature to 1200°C under dynamic heating conditions (10°C $min^{-1}$) and analysed in-situ using a Diffractometer Philips X'Pert Pro with a θ–θ goniometer and a high temperature chamber Anton Paar HTK-1200, the scanning rate used was 0.033° in the range 3–70 (2θ), with time constant of 15, 24 s and a detector X'Celerator. The measure conditions used were 1/8° for divergence slit and 1/4° for antiscattering slit, with a Cupper Anode at 40 kV and 40 mA.

## Results and discussion

### *Na-Vermiculite*

Figure 1a shows the X-ray diffraction pattern for the sample of vermiculite saturated in sodium (Na-V) and heated under static conditions at 900, 1000, 1100, 1200 and 1300°C, during one hour. Molten phase appears after heating at 1300°C. At 900°C the diffractions patterns are attributed to dehydrate Na-vermiculite (9.72, 4.56, 3.23, 2.45 Å, etc.) and to a starting new phase, nepheline (4.16, 3.83, 3.00, 2.88, 2.33 Å, etc.). After heating at 1000°C, nepheline phase is better developed and accompanied by forsterite (5.11, 3.88, 3.00, 2.76, 2.45 Å, etc.) as the predominant phase. At 1200 and 1300°C, the only phase present is forsterite. After heating at 1300°C, forsterite is accompanied by a glassy phase.

The X-ray diffraction patterns shown in Fig. 1b correspond to the Na-V heated up to 1200°C under dynamic conditions. In the range from 500 to 900°C, the diffraction peaks observed correspond to dehydrated sodium vermiculite (9.72, 4.53, 2.32 Å, etc.). At 1000°C two phases are formed, i.e. nepheline (4.16, 3.75, 3.00, 2.33, 1.57 Å, etc.) and forsterite (3.88, 3.73, 3.00, 2.45, 2.16 Å, etc.), coexisting with an amorphous phase. After heating at 1100°C, the nepheline phase disappears, being forsterite and an amorphous phase the only present phases. At 1200°C, the results are similar to those at 1100°C, appearing the forsterite phase well developed.

### *Cs-Vermiculite*

Figure 2a shows the X-ray diffraction pattern for the vermiculite saturated in cesium (Cs–V) and heated at

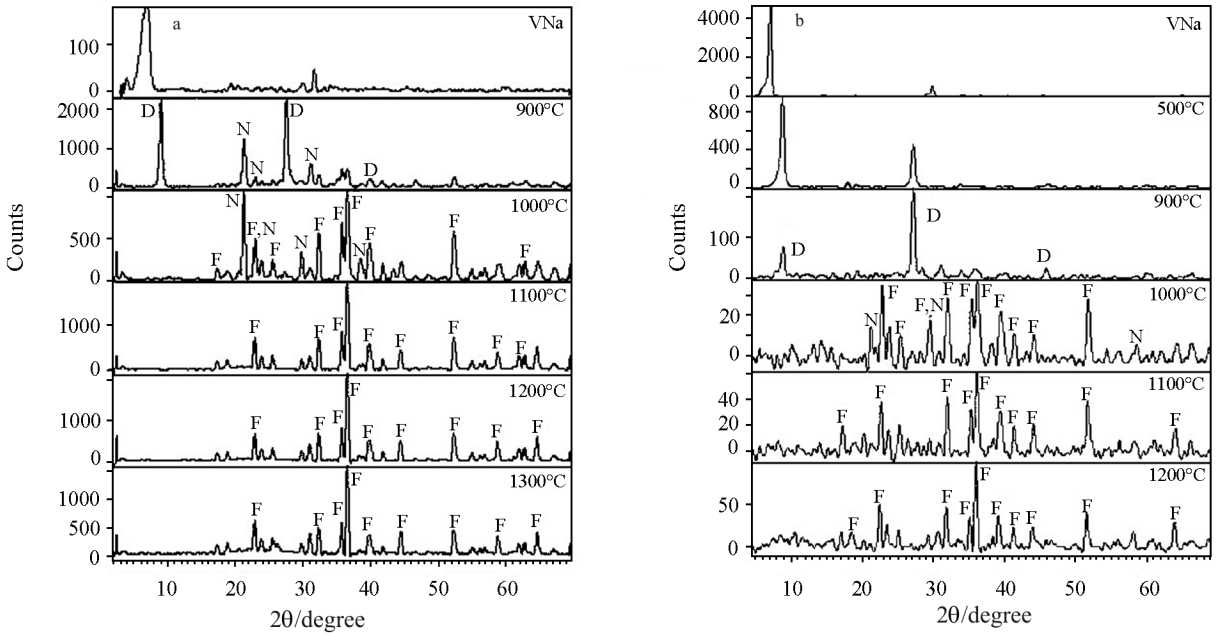


**Fig. 1** X-ray diffraction pattern at different temperatures for the a – Na-vermiculite heated under static and b – dynamic conditions. The identified phases are Forsterite (F), Nepheline (N) and dehydrated Na-vermiculite (D)

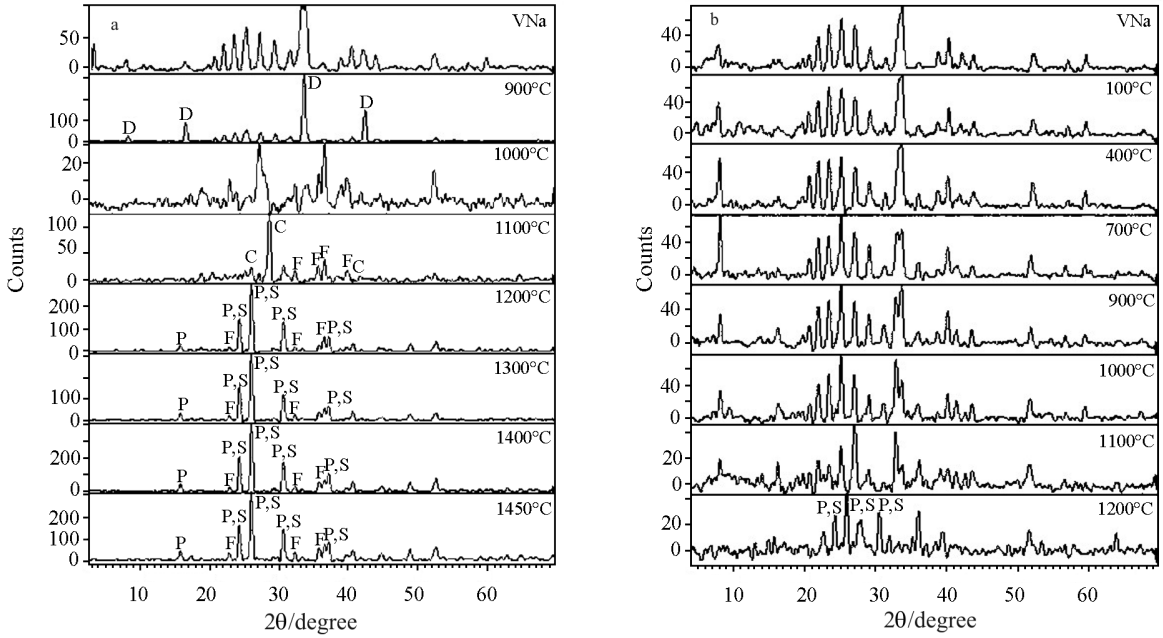


**Fig. 2** X-ray diffraction pattern at different temperatures for the a – Cs-vermiculite heated under static and b – dynamic conditions. The identified phases are dehydrated Cs-vermiculite (D), Coesite (C), Forsterite (F), Pollucite (P) and Cesium Magnesium Silicate (S)

900, 1000, 1100, 1200, 1300, 1400 and 1450°C under static conditions. At 900°C, diffractions at 10.65, 5.33, 3.25, 2.66, 2.12 Å, corresponding to dehydrated V–Cs, are present. At 1000°C, the intensity of the diffractions corresponding to the dehydrated phase significantly decreases. After heating at 1100°C, two new well developed phases are present, i.e. coesite (3.44, 3.10, 2.76, 2.19 Å, etc.) and forsterite (2.76, 2.51, 2.45, 2.26 Å, etc.), being also present an amorphous phase. At 1200°C, the sample suffers a drastic change; coesite disappears whereas forsterite is still present together with two new phases, pollucite (4.81, 3.65, 3.42, 2.90 Å, etc.) and cesium magnesium silicate (5.60, 3.42, 2.68, 2.42, 2.22 Å, etc.). The X-ray diffraction patterns of the sam-

ples heated at 1300, 1400 and 1450°C are similar to that of the sample heated at 1200°C, indicating that the formed phases are quite stable with temperature. At 1450°C the sample has melted forming a glassy phase together with pollucite, forsterite and cesium magnesium silicate.

Figure 2b shows the X-ray diffraction patterns for the sample Cs–V during the heating under dynamic conditions. Up to 1000°C, the original sample does not show changes and the diffraction peaks correspond mostly to the original vermiculite saturated with cesium. On heating at 1100°C, the V–Cs is still present but peaks related to pollucite and cesium magnesium silicate start to appear. At 1200°C, the only phases formed are pollucite (3.65, 3.42, 2.90 Å, etc.) and cesium magnesium silicate (3.66, 3.42, 2.68, etc.). These X-ray diffraction patterns show that these phases are less crystallized than under static heating.

### *$NH_4$–Vermiculite*

Figure 3a shows the X–ray diffraction pattern corresponding to the sample of vermiculite saturated with Ammonium ($NH_4$–V) heated at 900, 1000, 1100, 1200, 1300 and 1330°C under static conditions. At 900°C, diffractions were recorded at 6.27, 4.32, 3.13, 2.86, 2.49, 2.27, 2.08 Å attributed to enstatite, although slightly shifted as compared with the ASTM file values. Although, these shifts could suggest the substitution of Mg by Al and the presence of magnesium aluminium silicate, experiments at higher temperature indicate that the relative peak intensities and their positions are more in agreement with enstatite phase. At 1000°C, enstatite is the only phase formed. At 1200°C, spinel (2.85, 2.43, 1.55, 1.42 Å, etc.) also appears in minor proportion. After heating at 1300°C, a new phase, i.e. cordierite (8.45, 4.67, 4.09, 3.13, 2.65 Å, etc.), appears, being also present spinel and enstatite. The latter one is the predominant phase while the other phases increase their proportion with temperature. At 1330°C, the sample melted, appearing a glassy phase in addition to enstatite, spinel, cordierite and a new phase, forsterite (3.00, 2.45, 2.25, 1.94, 1.67 Å, etc.).

The sample of $NH_4$–V was heated under dynamic conditions up to 1200°C; the X-ray diffraction patterns are shown in Fig. 3b. The samples heated at 900, 1000, 1100 and 1200°C show diffraction peaks at 4.41, 3.15, 2.87, 2.53, 2.35 Å, etc., attributed to enstatite. At lower temperatures some diffraction peaks show a small shift in comparation with the ASTM files diffractions of enstatite, similarly as shown by static heating. This shift decreases and the peak intensities increase with temperature.

### *Mg–Vermiculite*

Figure 4a shows the X-ray diffraction pattern for the vermiculite sample saturated with magnesium (Mg–V) and heated during one hour at 900, 1000, 1100, 1200, 1300 and 1330°C, under static conditions. At 900 and 1000°C enstatite (3.15, 2.87, 2.49, 2.27 Å, etc.) is the only phase formed. At 1100, 1200 and 1300°C, enstatite is still present

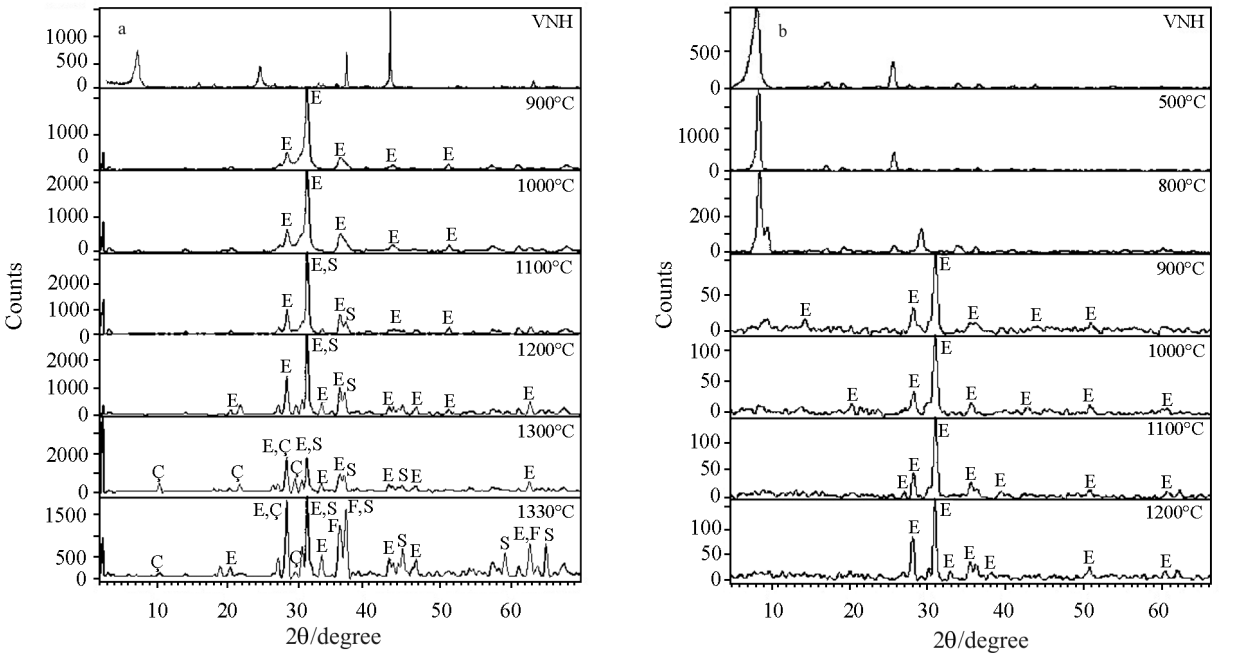


**Fig. 3** X-ray diffraction pattern at different temperatures for the a – $NH_4$-vermiculite heated under static and b – dynamic conditions. The identified phases are Enstatite (E), Spinel (S), Cordierite (C) and Forsterite (F)

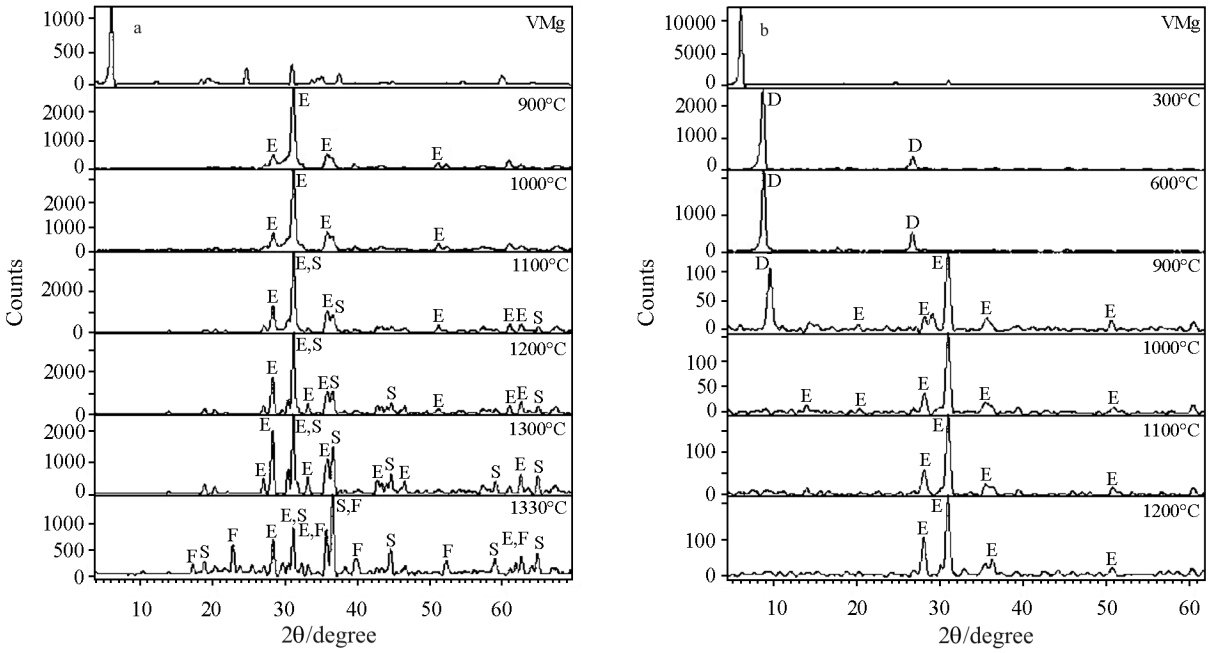


**Fig. 4** X-ray diffraction pattern at different temperatures for the a – Mg-vermiculite heated under static and b – dynamic conditions. The identified phases are Enstatite (E), Spinel (S) and Forsterite (F)

accompanied with spinel (2.85, 2.43, 2.02, 1.55, 1.42 Å, etc.) that appears better developed at the highest temperature. At 1330°C, enstatite and spinel still remain and a new phase appears, forsterite with diffractions at 5.10, 3.88, 3.73, 2.51, 2.44 Å, etc.

Figure 4b includes the diffraction pattern for the Mg–V heated under dynamic conditions up to 1200°C. The only phase formed was enstatite. At 900°C diffractions corresponding to dehydrate Mg–vermiculite (10.16, 5.03, 3.33, 2.45 Å, etc.) are present together with enstatite (4.41, 3.17, 2.87, 2.53, 2.27 Å, etc.). At 1000, 1100 and 1200°C, enstatite is the only phase formed and its diffraction intensities increase with the heating temperature.

*Ca–Vermiculite*

Figure 5a includes the X-ray diffraction patterns for the vermiculite sample saturated in calcium (Ca–V) and heated during one hour at 900, 1000, 1100 and 1200°C under static conditions. On heating at 900°C, some diffraction peaks attributed to enstatite (3.15, 2.87, 2.49, 2.46 Å, etc.) are detected, while their intensities increase after heating at 1000°C. At 1100°C a new phase, anorthite (4.68, 4.04, 3.62, 3.17, 2.52 Å, etc.) is developed, remaining enstatite that disappears completely at 1200°C. At this last temperature the sample melts, appearing a glassy phase and a new crystalline phase, forsterite (5.11, 3.88, 3.48, 3.00, 2.76, 2.51, 2.45 Å, etc.).

Figure 5b shows the X–ray diffraction pattern for the Ca–V heated up to 1200°C using dynamic conditions. At 900°C, few diffractions at 3.15, 2.87 and 2.53 Å, which fitted with those of the enstatite, are observed. At 1000°C the only phase formed is enstatite. On heating at 1100°C, the enstatite remains with the most intense peak at 2,87 Å, but a new phase appears, anorthite (3.91, 3.36, 3.19, 2.52 Å, etc.). Both phases are also detected at 1200°C.

*Ba–Vermiculite*

Figure 6a shows the X-ray diffraction pattern for the barium saturated vermiculite (Ba–V) heated under static conditions during one hour at 900, 1000, 1100 and 1200°C. After 900°C barium aluminium silicate (7.79, 3.94, 2.59, 2.19 Å, etc.) is well developed; the maximum peak situated at 2.87 Å, indicates that enstatite (3.15, 2.87, 2.49, 2.24, 1.97 Å, etc.) is starting to form, appearing completely developed at 1000°C. The phase barium aluminium silicate also appears at 1000°C, with more intense peaks than at 900°C and with the maximum at 7.79 Å. At 1100°C, the X-ray diffraction pattern is very closed to that at 1000°C, appearing the same phases, with enstatite in minor proportion than the silicate phase. After heating at 1200°C, both phases disappear while two new phases appear, celsian (6.52, 5.88, 4.61, 3.63, 3.47, 3.26 Å, etc.) and forsterite (5.11, 3.88, 3.00, 2.76, 2.26 Å, etc.), both of them with very intense diffractions.

Figure 6b shows the X-ray diffraction pattern for the Ba–V heated up to 1200°C under dynamic conditions. Before heating at 1000°C, diffractions at 10.04, 3.33, 2.64, 2.09 Å, etc. attributed to barium-vermicu-

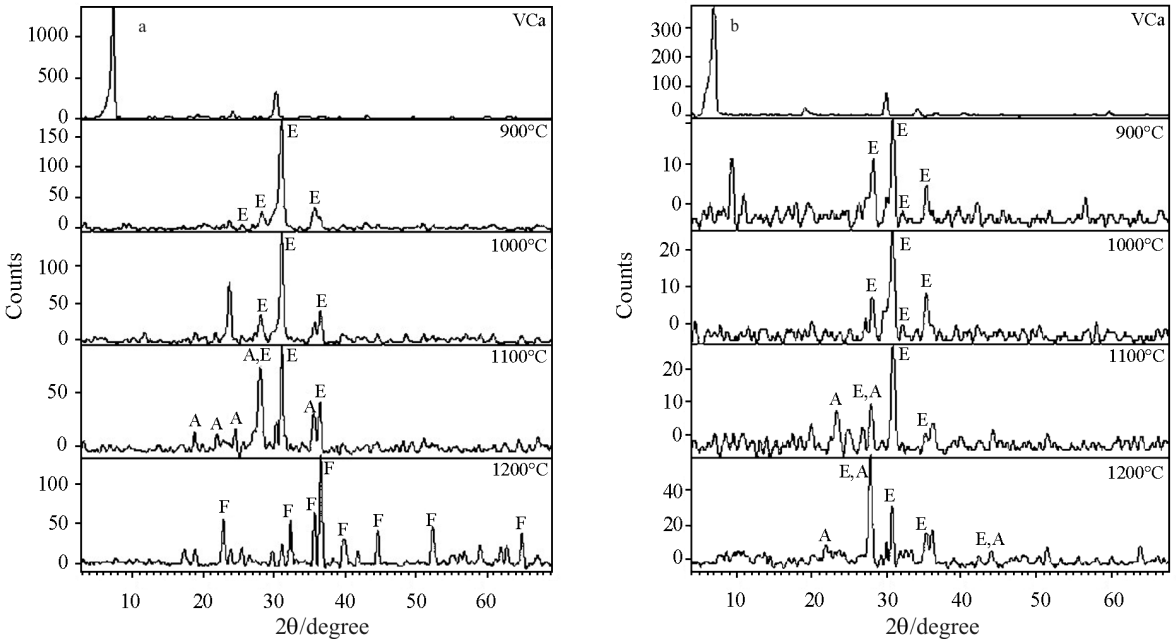


**Fig. 5** X-ray diffraction pattern at different temperatures for the a – Ca-vermiculite heated under static and b – dynamic conditions. The identified phases are Enstatite (E), Anorthite (A) and Forsterite (F)

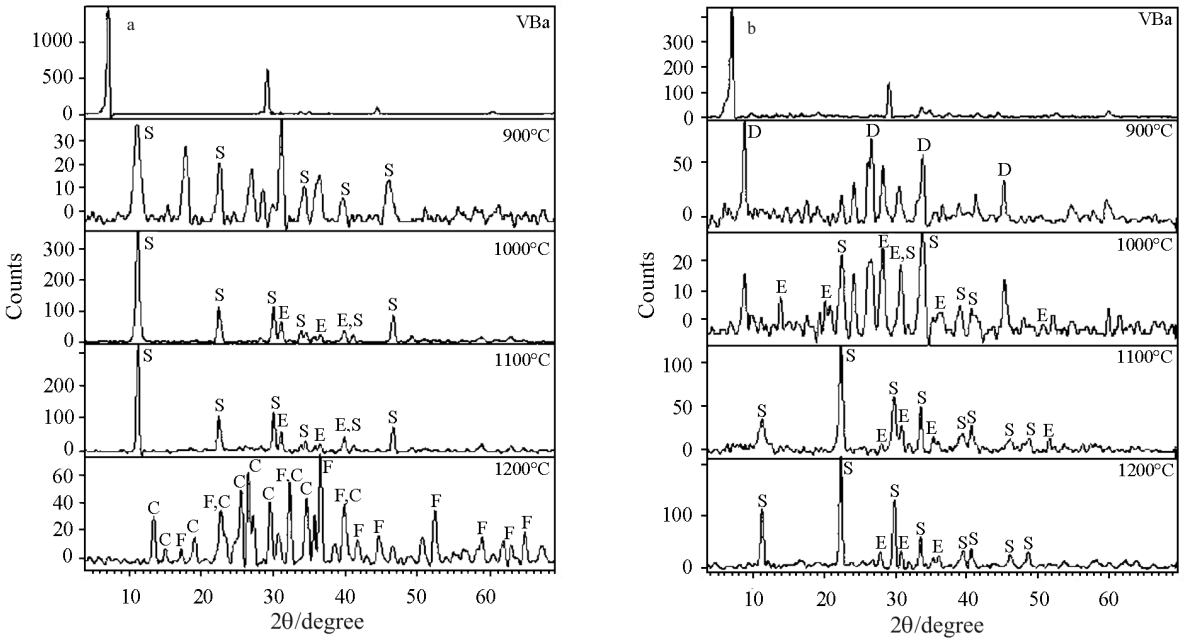


**Fig. 6** X-ray diffraction pattern at different temperatures for the a – Ba-vermiculite heated under static and b – dynamic conditions. The identified phases Enstatite (E), Forsterite (F), Celsian (C) and Barium Aluminium Silicate (S)

lite dehydrated are observed. At about 800°C, some other peaks of low intensity, which could indicate the formation of new phases are recorded. After heating at 1000°C, some peaks related to the dehydrated phase remain, appearing two new phases, barium aluminium silicate (3.94, 2.96, 2.64, 2.19 Å, etc.) and in minor proportion enstatite (6.33, 4.41, 3.15, 2.46 Å, etc.). At 1100 and 1200°C, the formed phases are also enstatite and barium aluminium silicate.

*Al–Vermiculite*

Figure 7a shows the X-ray diffraction pattern for the sample of vermiculite saturated with aluminium (Al–V) and heated under static conditions at 900, 1000, 1100, 1200 and 1300°C during one hour at each temperature. After heating at 900°C, diffractions corresponding to enstatite (6.33, 4.41, 3.15, 2.87, 2.49 Å, etc.) are observed, being the 2.87 Å the most intense

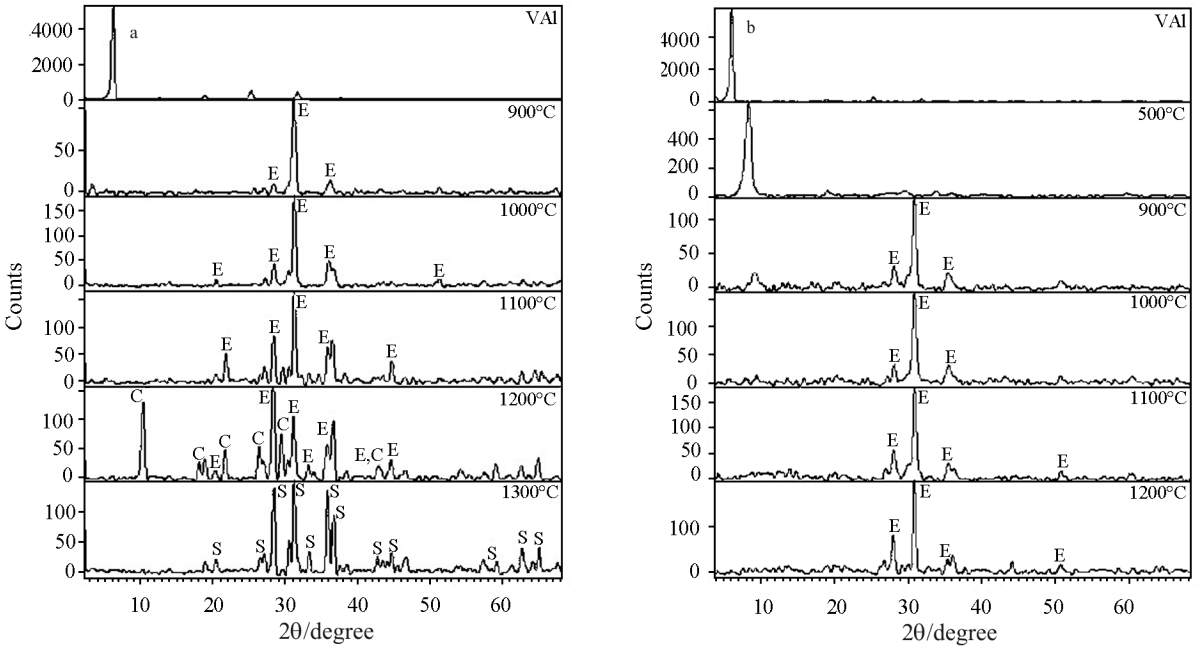


**Fig. 7** X-ray diffraction pattern at different temperatures for the a – Al-vermiculite heated under static and b – dynamic conditions. The identified phases are Enstatite (E), Cordierite (C) and Magnesium Aluminium Silicate (S)

peak. After heating at 1000 and 1100°C, the formed phase is also enstatite, but it is better developed. At 1200°C, cordierite (8.51, 4.67, 4.09, 3.38, 3.03, 2.65 Å, etc.) is recorded, but in less proportion than enstatite. Finally at 1300°C, these two phases disappear appearing a glassy phase as a consequence of the melting of the sample, together with a new well developed phase, magnesium aluminium silicate (4.32, 3.29, 3.13, 2.86, 2.69, 2.50, 2.45 Å, etc.).

Figure 7b shows the X-ray diffraction pattern for the Al–V heated under dynamic conditions up to 1200°C. At 900, 1000, 1100 and 1200°C the only present phase is enstatite (4.41, 3.17, 2.87, 2.53, 1.78 Å, etc.) while the peaks intensities increases with temperature.

Tables 1 and 2 include the phases formed for the vermiculite saturated with different cations heated under static and dynamic conditions, respectively. In general, some differences are found for static and dynamic heating experiments. Thus, the phases formed are better developed under static heating at lower temperatures and some phases are formed only under static heating. Thus, for Na–V, nepheline appeared at 900 and 1000°C under static and dynamic heating, respectively; this phase was better defined for static conditions. For Cs–V, under static heating, coesite (1100°C) and forsterite (1200–1450°C) are detected only under static heating. For $NH_4$–V, phases like cordierite, spinel and forsterite, are detected under static heating but not under dynamic heating. Similarly, for Mg–V, spinel and forsterite are only detected under static conditions. For the Ca–V, the enstatite and anorthite phases are transformed into forsterite only for the sample heated under static conditions. For the Ba–V, the enstatite and barium aluminium silicate are transformed into celsian and forsterite only for the static heating. For the Al–V sample, under static heating at 1200°C, appears a new phase, cordierite, in similar proportion than enstatite that is not present in the sample heated under dynamic conditions.

This study has shown that the main phases observed for vermiculite are enstatite and forsterite. Other phases, such as spinel, cordierite, pollucite, nepheline, etc., are also observed for some of the samples. Crystal phases are determined by the different cations in the interlayer space. Thus, nepheline is only observed when sodium is present in the structure, that is in the sodium vermiculite. Pollucite and cesium magnesium silicate appear only for the cesium vermiculite. Barium aluminium silicate and magnesium aluminium silicate are registered only for barium vermiculite and magnesium vermiculite, respectively. Heating conditions (static or dynamic) have a significant influence on the temperature at which the phases are observed; even some phases could not be detected under dynamic heating. The behaviour observed in this study can be understood considering the complexity of the studied system. Thus, the $SiO_2$–$Al_2O_3$–MgO phase diagram [24] shows that for the chemical composition of vermiculite, different phases, such as enstatite, forsterite, spinel, cordierite, are present in a narrow composition range. All these phases have been

**Table 1** Phases formed during static heating of vermiculite saturated with different cations

| *T*/°C | Na–V | Cs–V | $NH_4$–V | Mg–V | Ca–V | Ba–V | Al–V |
|---|---|---|---|---|---|---|---|
| 900 | NaV deh[1] Nepheline | CsV deh[1] | Enstatite | Enstatite | Enstatite | BaAlSil[2] | Enstatite |
| 1000 | Forsterite Nepheline | CsV deh[1] | Enstatite | Enstatite | Enstatite | BaAlSil[2] Enstatite | Enstatite |
| 1100 | Forsterite | Coesite Forsterite | Enstatite Spinel | Enstatite Spinel | Enstatite Anorthite | BaAlSil[2] Enstatite | Enstatite |
| 1200 | Forsterite | Pollucite Forsterite CsMgSil[3] | Enstatite Spinel | Enstatite Spinel | Forsterite Glassy | Celsian Forsterite Glassy | Enstatite Cordierite |
| 1300 | Forsterite Glassy | Pollucite Forsterite CsMgSil[3] | Enstatite Cordierite Spinel | Enstatite Spinel | | | MgAlSil[4] Glassy |
| 1330 | | | Enstatite Spinel Cordierite Forsterite Glassy | Enstatite Forsterite Spinel Glassy | | | |
| 1400 | | Pollucite Forsterite CsMgSil[3] | | | | | |
| 1450 | | Pollucite Forsterite CsMgSil[3] Glassy | | | | | |

[1]deh=dehydroxylated, [2]BaAlSil=Barium Aluminium Silicate, [3]CsMgSil=Cesium Magnesium Silicate, [4]MgAlSil=Magnesium Aluminium Silicate

**Table 2** Phases formed during dynamic heating of vermiculite saturated with different cations

| T/°C | Na–V | Cs–V | $NH_4$–V | Mg–V | Ca–V | Ba–V | Al–V |
|---|---|---|---|---|---|---|---|
| 900 | NaV deh[1] | CsV | Enstatite | Enstatite | Enstatite | BAV deh[1] | Enstatite |
| 1000 | Forsterite Nepheline | CsV | Enstatite | Enstatite | Enstatite | BaAlSil[2] Enstatite | Enstatite |
| 1100 | Forsterite | Pollucite CsMgSil[3] | Enstatite | Enstatite | Enstatite Anorthite | BaAlSil[2] Enstatite | Enstatite |
| 1200 | Forsterite | Pollucite CsMgSil[3] | Enstatite | Enstatite | Enstatite Anorthite | BaAlSil[2] Enstatite | Enstatite |

[1]deh=dehydroxylated, [2]BaAlSil=Barium Aluminium Silicate, [3]CsMgSil=Cesium Magnesium Silicate

detected in our study. Stoch [22] has also observed when studying the crystallization of $SiO_2$–$Al_2O_3$–MgO glasses the formation of solid solutions and a multistage crystallization where enstatite is formed first, followed by the crystallization of forsterite and cordierite. In our samples, enstatite is also the phase firstly formed for all the samples except Na–V and Cs–V, where enstatite is not formed and forsterite is the first phase detected. Additionally, the presence of the interlayer cation, explains the formation of some specific phases where the interlayer cation is involved. Finally, the experimental conditions are not necessarily in equilibrium and, therefore, kinetics plays a role.

## Acknowledgements

This publication was prepared on the basis of the results obtained in the fame of the projects MAT2005-04838 and MAT2004-02640 supported by the Ministry of Education and Science of Spain.

## References

1 A. Russell, Vermiculite Industrial Minerals Annual Supplement London V. 332 8496, September 3, 1998, p. 8.
2 M. J. Potter, Am. Ceram. Soc. Bull., 78 (1999) 145.
3 P. Couderc and Ph. Douillet, Bull. Soc. Fr. Ceram., 99 (1973) 51.

4 E. M. Dickson, Insulating refractories – Vermiculite, perlite and diatomite rocks palying and increasing role. Ind. Miner. Refractories Survey, 1981, pp. 151–157.
5 D. G. H. Ballard and G. R. Rideal, J. Mater. Sci., 18 (1983) 545.
6 P. H. Nadeau, Appl. Clay Sci., 2 (1987) 83.
7 J. R. Hindman, Vermiculite in Carr, D. D., Sr. Ed., Industrial minerals and rocks: Littleton, Co., Society for Mining, Metallurgy and Exploration, Inc. 1994, pp. 1103–1111.
8 P. W. Harben, The Industrial Minerals Handbook. Industrial Minerals Division Metal Bulletin PLC London 1995, United Kingdom.
9 W. F. Ford, The Effect of Heat on Ceramic. Macularen and Sons Ltd., London 1967.
10 J. M[a] Rincón López, Bol. Soc. Esp. Cerám. Vidrio, 23 (1984) 97.
11 J. M[a]. Rincón López, Bol. Soc. Esp. Cerám. Vidrio, 23 (1994) 171.
12 J. Podebradska, R. Cerny, J. Drchalova, P. Rovnanikova and J. Sestak, J. Therm. Anal. Cal., 77 (2004) 85.
13 I. Barshad, Amer. Miner., 35 (1950) 225.
14 H. G. Reichenbach and J. Bayer, Clay Miner., 29 (1994) 327.
15 G. F. Walter and W. F. Cole, The Vermiculite Minerals in: The Differential Thermal Investigation of Clays. R. C. Mackenzie, Ed., Mineralogical Society, London 1957, pp. 191–206.
16 R. C. Mackenzie, Simple Phyllosilicates Based on Gibbsite and Brucita-like Sheets in: Differential Thermal Analysis. R. C. Mackenzie Ed., Academia Press, London 1970, pp. 498–534.
17 L. A. Perez-Maqueda, V. Balek, J. Poyato, J. L. Perez-Rodriquez, J. Subrt, I. M. Bountsewa, I. N. Beckman and Z. Malek, J. Therm. Anal. Cal., 71 (2003) 715.
18 J. Poyato, L. A. Perez-Maqueda, M. C. Jimenez De Haro, J. L. Perez-Rodriguez, J. Subrt and V. Balek, J. Therm. Anal. Cal., 67 (2002) 73.
19 J. Poyato, L. A. Perez-Maqueda, A. Justo and V. Balek, Clays Clay Miner., 50 (2002) 791.
20 L. A. Perez-Maqueda, J. Poyato and J. L. Perez-Rodriguez, J. Therm. Anal. Cal., 78 (2004) 375.
21 G. F. Walker, X-ray Identification and Crystal Structures of Clay Minerals. Chapter 7. G. W. Brindley, Mineralogical Society, London 1951, pp. 199–223.
22 L. Stoch, J. Therm. Anal. Cal., 77 (2004) 7.
23 L. A. Perez-Maqueda, O. B. Caneo, J. Poyato and J. L. Perez-Rodriguez, Phys. Chem. Miner., 28 (2001) 61.
24 W. Shreyer and J. F. Schairer, J. Petrol., 2 (1961) 325.

DOI: 10.1007/s10973-005-7194-6